FOG-Aleut-2F Rec'd 4/15/05

Spatial and Temporal Variability of the Aleutian Climate

SERGEI N. RODIONOV[1*], JAMES E. OVERLAND[2] AND NICHOLAS A. BOND[1]

[1]*University of Washington, JISAO, Seattle, WA 98195, USA*
[2]*NOAA, Pacific Marine Environmental Laboratory, Seattle, WA 98115, USA*

Running title: *Aleutian Climate Variability*

To be published in *Fisheries Oceanography*

Revised July 1, 2004

[*] *Correspondence.* E-mail: Sergei.Rodionov@noaa.gov, tel..: 206-526-6211, fax: 206-526-6485.

ABSTRACT

The objective of this paper is to highlight those characteristics of climate variability that may pertain to the climate hypothesis regarding the long-term population decline of Steller sea lions (*Eumetopias jubatus)*. The seasonal changes in surface air temperature (SAT) across the Aleutian Islands are relatively uniform, from 5-10˚C in summer to near freezing temperatures in winter. The interannual and interdecadal variations in SAT, however, are substantially different for the eastern and western Aleutians, with the transition found at about 170˚W. The eastern Aleutians experienced a regime shift toward a warmer climate in 1977, simultaneously with the basin-wide shift in the Pacific Decadal Oscillation (PDO). In contrast, the western Aleutians show a steady decline in winter SATs that started in the 1950s. This cooling trend was accompanied by a trend toward more variable SAT, both on the inter- and intra-annual time scale. During 1986-2002, the variance of winter SATs more than doubled compared to 1965-1985. At the same time in southeast Alaska, the SAT variance declined in half. Much of the increase in the intra-seasonal variability for the western Aleutians is associated with a warming trend in November and a cooling trend in January. As a result, the rate of seasonal cooling from November to January has doubled since the late 1950s. We hypothesize that this trend in SAT variability may have increased the environmental stress on the western stock of Steller sea lions and hence contributed to its decline.

KEY WORDS: Aleutian Islands, Aleutian low, regime shift, sea level pressure, storm tracks, surface air temperature, trend, 500-hPa height.

INTRODUCTION

From a climatological viewpoint the Aleutian Islands are a key area where one of the most prominent atmospheric centers of action – the Aleutian low – is located. The Aleutian low and its effect on the North Pacific climate is a subject of numerous publications (Seckel, 1993; Trenberth and Hurrell, 1994; King at al., 1998; Overland et al., 1999; Miller and Schneider, 2000; Chang and Fu, 2002). Regional climatic fluctuations in such areas as the Sea of Okhotsk (Tachibana et al., 1996), Bering Sea (Niebauer 1998) and Gulf of Alaska (Flatau et al., 2000) are often linked directly to the strength and position of the Aleutian low. These and other studies notwithstanding, the climate of the Aleutian Islands themselves has received little scientific attention, as evidenced by the lack of any entries specifically on this topic in *Meteorological and Geoastrophysical Abstracts*. In particular, the spatial and temporal variability of the climate of the Aleutians is not well known, yet these variations are apt to be important to the marine ecosystem of the region.

The population of Steller sea lions (*Eumetopias jubatus*) in the Aleutian Islands has experienced a steep decline, and it has been hypothesized that this decline may be related to changes in climate (Springer 1998; Benson and Trites 2002). Declines have been apparent in all areas west of 144˚W (western stock), although not at the same rate. The exact timing of declines in each area is difficult to establish because frequent (on schedule of about every 2 years) range-wide counts did not begin until 1989 (NRC 2003). A decline was first observed in the eastern Aleutian Islands; Braham *et al*. (1980) estimated the decline in this area of at least 50% from 1957 to 1977. By 1985, population declines had spread throughout the Aleutian Islands and eastward into the Gulf of Alaska

(NRC 2003). There is some evidence that the most dramatic decline occurred between 1985 and 1989 and that this rapid decline included the entire western stock (York et al. 1996). Since 1989, the rates of declines have lessened in most areas of the western stock, with stabilizing populations at very low levels (NRC 2003). Overall, the western stock is declining at about 5% per year, and total population numbers have dropped by over 80% since the late 1960s (Loughlin and York 2000).

The goal of this paper is not to identify a mechanism that links changes in climate and sea lion population dynamics, which would be premature given the state of our knowledge on the subject. Instead, our primary objective here is to document major aspects of the climate variability (trend, regime shifts, etc.) that can be *potentially* used to substantiate the climate hypothesis on the sea lions decline, leaving the explanation itself for further research. One of the least ambiguous parts of this decline is that it is confined to the western stock. In contrast, populations of the eastern stock (east of 144˚W from Southeastern Alaska to California) are relatively stable and sea lion population there is even increasing (Fig. 1). Therefore, the primary objective of this paper is to document the climate variability in the region of the western stock, in particular, the Aleutian Islands. Much of the analysis focuses on the differences that have occurred in the western versus eastern portion of the Aleutians.

Our description of the climate variability of the Aleutian Islands includes considerable information on the corresponding variability of the atmospheric circulation. Anomalies in the atmospheric circulation cause surface air temperature anomalies directly through variations in the horizontal advection of heat but also contribute in less direct ways. Atmospheric circulation anomalies impact the distribution of clouds and

temperature and humidity profiles aloft and therefore also shortwave and longwave radiative fluxes at the surface. In general, anomalies in the net radiative fluxes at the ocean surface in the middle to high latitudes during the cool season have the same sign as those for the sensible and latent heat fluxes, and hence affect the sea surface temperature (SST) in the same sense. In turn, SST has subsequent feedbacks on surface air temperature through its modulation of surface sensible heat fluxes. It is beyond the scope of this analysis to detail how the low-level advection of heat, effects of SST and net radiative heat fluxes have varied from year to year. The important point for the purpose of this study is that these effects tend to act in concert in determining the mean surface air temperature in a particular season, and that they are all related to the anomalous atmospheric circulation.

Due to the scarcity of direct meteorological and oceanographic observations in the Aleutian Islands region, our analysis heavily relies on the National Centers for Environmental Prediction (NCEP) - National Center for Atmospheric Research (NCAR) Reanalysis data (Kalnay et al. 1996). Although the reanalysis system assimilates efficiently upper air observations, it is only marginally influenced by surface observations because the model orography is quite different than the real detailed distribution of mountains and valleys. Furthermore, the 2m-temperature analysis is strongly influenced by the model SST and parameterization of energy fluxes at the surface. Nevertheless, a comparison of monthly mean 2m-temperature produced by the NCEP/NCAR reanalysis with the surface analysis based purely on land and marine 2m surface temperature observations shows very good correspondence (Kistler et al. 2001). Throughout the

paper, if the data source is not explicitly specified, NCEP-NCAR Reanalysis should be assumed.

We will start with a brief description of the background climatic characteristics of the Aleutian climate. The next section will examine the range of variability associated with the extreme states of the Aleutian low. It will be followed by a more detailed look at the atmospheric variability in the western and eastern Aleutian Islands including analysis of the climatological transition between these two regions. Next, we will present the trend analyses of atmospheric circulation and surface air temperature (SAT). Changes in both mean level and variance over time will be considered. And finally, we will discuss the regional manifestations of the regime shifts of 1977 and 1989. Our findings may shed some light on the role of the environment in the decline of Steller sea lions.

BACKGROUND CLIMATIC CONDITIONS

The Aleutians are a chain of small islands that separate the Bering Sea (north) from the main portion of the Pacific Ocean (south) and extend in an arc southwest, then northwest, for about 1800 km from the tip of the Alaska Peninsula to Attu Island, Alaska, U.S. (Fig. 2). The islands experience a cool, wet, and windy maritime climate. Typical summertime temperatures are in the range of 5-10˚C, and winter temperatures are around freezing. Precipitation varies widely, from 530 mm up to 2,080 mm. Wind, light rain, and fog are common in the summer, but the wettest conditions generally occur during October-December.

The islands gave the name to one of the most prominent centers of atmospheric action, the Aleutian low. It is strongest in winter and practically disappears in summer. In winter (defined here as December through February), the long-term mean position of the Aleutian low is located at about 52˚N and slightly west of the dateline (Fig. 3a). This is the position where storms typically reach their lowest pressure. It does not mean, however, that the storms here are most frequent. Nor does it mean that the sea-level pressure (SLP) distribution in Fig. 3a is the most typical atmospheric circulation pattern in the region. As we will see below, this pattern is rather a statistical combination of two distinct patterns. One pattern represents the Aleutian low centered *east* of the dateline, and the other features a split Aleutian low with one center east of Kamchatka Peninsula, and the other in the Gulf of Alaska.

In the middle troposphere (the 500-hPa level) the atmospheric circulation is characterized by a climatological trough along the East Asian coast and ridge along the west North American coast (Fig. 3b). Their mean positions are attributable to such

"stationary" factors as the earth's orography and geographic distribution of the oceans and continents. Other factors, however, such as surface temperature, distribution of snow and ice, internal atmospheric dynamics, and remote influences, cause significant interannual and longer-term variations in the both position and strength of the East Asian trough and North American ridge. Our analysis shows that variability in the position of the North American ridge is about twice as much as that of the East Asian trough. Although the North American ridge tends to strengthen (weaken) as the East Asian trough becomes deeper (shallower), the correlation between the two is rather weak, and it is reasonable to say that they are relatively independent. Their combined variability determines the direction of the Pacific storm track.

Storms typically originate east of Japan and move northeastward along the Aleutian chain to the Gulf of Alaska (Fig. 3c). There is a secondary storm track along the Asian coast to the western Bering Sea. The direct exposure of the Aleutian Islands to passing storms results in the frequent occurrence of winds in excess of 22 ms^{-1} (50 mph) during all but the summer months. The Gulf of Alaska usually is a "graveyard" for storms, but occasionally, cyclogenesis can also occur there. Therefore, this is the area where cyclones are most frequent. The arrows in Fig. 3c indicate the stability of storm trajectories. The shorter the arrow, the less stable is the direction of storms passing through that area. In the area of cyclogenesis east of Japan the lengths of the arrows are close to the standard unit length, which indicates that all the storms move in the direction pointed by the arrow. In contrast, in the Gulf of Alaska the arrows are shorter, which means that storms come here from a variety of directions. Note also a "gap" between these two areas of high frequency of storms. This gap is a result of high variability of the latitudinal position of

the storms track between 170˚W and 150˚W. It is not surprising therefore, that SLP variability reaches its maximum in the area south of the Alaska Peninsula.

RANGES OF VARIABILITY

Since temperature variations in the Aleutian Islands are primarily determined by the Aleutian low, it is instructive to examine two opposite climatic situations associated with the extreme states of the Aleutian low. A widely used measure of the strength of the Aleutian low is the North Pacific (NP) index introduced by Trenberth and Hurrell (1994). The index is the area-weighted SLP over the region 30˚N-65˚N, 160˚E-140˚W. Positive (negative) values of the index indicate a weak (strong) Aleutian low. The time series of this index for the period 1950-2003 is presented in Fig. 4. During this period, the index exhibits a strong negative trend, which is statistically significant at the probability level $p = 0.01$[*]. This decline, however, was not monotonic. In the late 1970s, the NP index, along with other climatic variables (see Regime Shifts below), experienced an abrupt shift from predominantly positive values before 1977, to predominantly negative values since then. According to the Student's t-test (two-tail assuming unequal variances), the difference in the mean index values for 1950-1976 and 1977-2003 is statistically significant at $p = 0.0008$.

To characterize the atmospheric circulation and SAT anomalies associated with a strong Aleutian low, we constructed composite maps for 10 winters (DJF) with the lowest NP index values during 1950-2003 (Fig. 5). Note that 6 of these winters occurred within the 11-year period from 1977 through 1987. The composite map for SLP (Fig. 5a) shows that the Aleutian low is shifted eastward and its central pressure is 6 hPa lower compared to the climatology (Fig. 3a). The area of the strongest negative SLP anomalies (Fig. 5b) is

[*] Significance of a trend was determined as the significance of the regression coefficient when the variable is linearly regressed on time. The effective number of degrees of freedom was estimated using the formula in Bayley and Hammersley (1946).

centered south of the Alaska Peninsula, that is, where the SLP variability is the highest. Nevertheless, normalized SLP anomalies in that area exceeded one standard deviation and, hence, where statistically significant at $p < 0.01$.

The composite for 500-hPa heights (Fig. 5c) indicate a deeper East Asian trough extended south-eastward and a stronger North American ridge compared to the climatology (Fig. 3b). The most significant negative anomalies at the 500-hPa level are found approximately in the same place as those at the surface, which indicates that the atmosphere over the North Pacific can be considered as equivalent barotropic. Strong gradients to the south and east of this center of negative anomalies suggest anomalously strong westerly winds in the subtropical latitudes and south-easterly winds along the North American coast.

Reflecting those changes in the mean geostrophic flow, the storm track is shifted southward in the central North Pacific (Fig. 5c). The anomalously strong North American ridge blocks the storms from entering the continent steering them north-eastward into the Gulf of Alaska. Some storms may turn northward even earlier, hitting the central and eastern Aleutian Islands. Note that the number of storms entering the Bering Sea along the Asian coast is greatly reduced.

The SAT anomaly pattern (Fig. 5f) closely resembles the loading pattern for the Pacific Decadal Oscillation (PDO), which is the leading principal component of North Pacific monthly sea surface temperature variability poleward of 20˚N (Mantua et al. 1997). The center of negative SAT anomalies is positioned to the west-south-west of the center of negative 500-hPa anomalies (Fig. 5d). These negative SAT anomalies are associated with an advection of cold air produced by anomalous north-westerly

geostrophic winds in the region. Overall, this atmospheric circulation is considered to be zonal because of the stronger-than-average north-south pressure gradient in the mid-latitudes (cf. Figs. 3b and 5c), and hence, stronger westerly winds. Under this type of circulation, a number of processes contribute to cooling of SSTs in the western and central North Pacific: 1) enhanced sensible and latent heat fluxes from the ocean to the atmosphere, 2) greater wind mixing of cool water from depth to the surface, 3) southward Ekman transport and 4) anomalous mid-ocean upwelling. The thermal damping theory proposed by Barsugli and Battisti (1998) indicates that in the extratropics, ocean-atmosphere coupling decreases the energy flux between the two media. This adjustment results in a reduction of the effective thermal damping of the ocean on the atmosphere, lengthening the persistence of the anomalies.

Positive SAT anomalies along the west coast of North America are also associated with an advection of warm air from the south. This warm and moist air reduces sensible and latent heat flow from the ocean to the atmosphere, so that both media maintain positive temperature anomalies. The Aleutian Islands are also warmer than the 50-yr norm (1951-2000), but the magnitudes of the anomalies become progressively smaller from east to west.

A set of composite maps for 10 years with the highest values of the NP index is presented in Fig. 6. Six of those years occurred in the 1950s and none in the 1990s. The Aleutian low is not only weak in those years it is split into two centers, with the main center east of Kamchatka Peninsula and the secondary center in the Gulf of Alaska (Fig. 6a). Note also a well developed eastern Subtropical high. SLP anomalies are positive over virtually the entire North Pacific (Fig. 6b).

At the 500-hPa level a strong anomalous ridge is situated over the east-central North Pacific extending into the Bering Sea (Fig. 6c). The 500-hPa anomaly pattern (Fig. 6d) is almost a mirror image of the low pressure cell in Fig. 5d, except that the positive anomalies in the central Pacific extend farther north into the Chukchi Sea. As a result, the anomalous geostrophic flow over the Aleutians is not opposite to that during the years with low values of the NP index.

Due to an anomalous ridge over the North Pacific, cyclones infrequently cross the ocean; many of them are steered northward prior to reaching the dateline (Fig. 6e). An increased frequency of storms moving along the secondary storm track enhances the advection of warm subtropical air to the western Aleutians. As the result, winters there are warmer than the 50-yr norm with positive SAT anomalies on the order of 0.4-0.6 standard deviations (Fig. 6f). The Gulf of Alaska still remains one of the most prominent centers of cyclonic activity, but the majority of storms are now coming from the west and north-west (Fig. 6e), rather then from the south-west as during years with low values of the NP index (Fig. 5e). The advection of Arctic air behind the cold fronts of those storms and the mean north-westerly anomalous flow bring about below normal temperatures in the extreme eastern Aleutians. Thus, under the type of circulation associated with a weak Aleutian low, the temperature contrast between the western and eastern Aleutian Islands is more pronounced. The next section takes a closer look at the differences in atmospheric variability between the western and eastern Aleutians.

VARIABILITY IN THE EASTERN AND WESTERN ALEUTIANS

Due to the lack of meteorological stations in the Aleutian Islands with consistent records of observation, two nearby stations, Nikolskoe (55.2˚N, 166.0˚E), Commander Islands and Cold Bay (55.2˚N, 162.7˚W) at the tip of Alaska Peninsula (Fig. 2), were chosen to characterize climate variability of the western and eastern parts of the Aleutian chain, respectively. To justify the use of these stations, we calculated the spatial correlations in the winter (DJF) SAT field using these stations as the base points (Fig. 7). For Nikolskoe (Fig. 7a), the area of the correlation coefficients greater than 0.7 extends eastward to about the dateline. Farther eastward the correlation coefficients quickly decrease, becoming zero near Cold Bay, and then turn negative in the Gulf of Alaska and western Canada. The correlation pattern for Cold Bay (Fig. 7b) is practically orthogonal to that for Nikolskoe (Fig. 7a). It is important to note that both maps suggest an existence of a zone near 170˚W that represents a transition region between the west and east in terms of the climate fluctuations of the Aleutians. More about this zone will be discussed later.

In addition to SAT, we use three other meteorological variables to characterize atmospheric circulation: surface zonal (U) and meridional (V) wind components and momentum flux (stress). The time series for the wind components were extracted from the mean monthly NCAR/NCEP Reanalysis data set (Kalnay et al. 1996) for the grid points 55˚N, 165˚E and 55˚N, 165˚W. The wind stress was calculated for the same grid points using daily Reanalysis data. The magnitude of the surface wind stress is approximately proportional to the wind speed squared, and is also roughly proportional to the height of surface waves (in a fully developed sea). This wind stress index is more sensitive to the frequency and intensity of the occasional strong storm than the day-to-day

variations in the winds. Fig. 8 shows seasonally averaged time series of all these meteorological variables for three seasons: yearly winter (November-December), late winter (January through March), and spring (April-May).

November-December (Fig. 8, Top Panel)

In November-December, the long-term mean value of the zonal (u) wind speed at Nikolskoe is about zero, which means that the westerly winds here are about as frequent as the easterly winds. At Cold Bay, westerly winds slightly dominate. The year-to-year variations in the zonal wind speed at these two locations are correlated at $r = 0.55$, which is significant at the probability level $p < 0.01$ (one-tail). Both locations experienced enhanced variability in the zonal wind in the mid-1990s. In November-December 1995, the easterly winds at Nikolskoe were the strongest for the entire period considered here, and those at Cold Bay were the second strongest (after 1980). In November-December 1997 (the year of a strong El Niño event), both locations experienced the strongest westerly winds.

The meridional (v) wind components at Nikolskoe and Cold Bay tend to fluctuate out-of-phase, which can be expected given the positions of these stations at the eastern and western periphery of the Aleutian low respectively (Fig. 3a). The correlation coefficient between these two variables is only moderately negative ($r = -0.33$), but still significant at $p = 0.05$. An extreme case of this opposition was observed in November-December 2000, when Nikolskoe and Cold Bay had the strongest northerly and southerly winds during the period of record, respectively. At Cold Bay, this year was particularly unusual because the period of 1995-2002 was characterized by anomalous northerly winds in general, with the record strong northerly wind component observed in 1999.

The wind stress index suggests that it was relatively stormy at Nikolskoe during the period 1965-1977. As shown in the previous section, this was probably associated with high frequency of storms along the secondary storm track (Fig. 6e) directed toward the western Aleutians. The climate shift in the North Pacific in the late 1970s toward a new regime of stronger Aleutian low (Miller et al. 1994) was also characterized by a southward shift in the storm track, away from the Western Aleutians similar to that shown in Fig. 5e. This suggests that this region should have experienced a sharp decline in the degree of storminess. In fact, according to the Student's t-test (two-tail), the difference in the mean values of the wind stress index between 1965-1977 and 1978-1992 is statistically significant at $p = 0.004$. This relatively calm period continued until 1992 when the wind stress index increased again to pre-1978 levels. Statistically, the difference between the mean values of the index for 1978-1992 and 1993-2002 is highly significant ($p = 0.003$). At Cold Bay, the wind stress index also experienced a shift in the late 1970s, but in the opposite direction compared to that in Nikolskoe, that is, from a relatively calm period 1956-1976 to a stormier period 1977-2001. The index difference between these two periods is statistically significant at $p = 0.04$. This shift in the index is consistent with the redistribution of the storm track, with more storms battering the Eastern Aleutians after the climate shift in the late 1970s (Fig. 5e) than before (Fig. 6e).

The variability in SAT at Nikolskoe was relatively large in the 1980s and 1990s. The warmest early winter season here was observed in 1995, when the SAT anomaly was +3.1˚C, which exceeds three standard deviations. This anomaly was caused by an extremely strong easterly winds, as noted above, that brought warm Pacific air into the region. It is interesting that extremely strong northerly winds in November-December

2000 did not cause a marked decline in SAT. The reason is that these northerly winds were associated with an abnormally strong low pressure cell over the central Aleutian Islands and counter-clockwise circulation of relatively warm Pacific air around this cell and not with advection of cold Arctic or Siberian air. This demonstrates that not all northerly winds are alike and explains why the correlation coefficient between SAT and meridional wind at Nikolskoe (r = 0.54) is not as strong as one might expect. In contrast, variations in SAT at Cold Bay are closer linked to those in meridional wind (r = 0.69). Negative SAT anomalies dominated this region from 1956 through 1977, and positive SAT anomalies thereafter, with one prominent exception of 1999, which was the coldest year in the time series. The difference in SAT between 1956-1977 and 1978-1996 is statistically significant at p = 0.002.

January – March (Fig. 8, Middle Panel)

In January – March, the major storm track lies to the south of the Aleutian Islands and zonal winds at both Nikolskoe and Cold Bay are mostly from the east. The correlation coefficient between zonal winds at these two locations (r = 0.40) is less strong than that during November-December. There were two periods at Cold Bay, 1964-1969 and 1999-2002, that are characterized by anomalous westerlies. An analysis of SLP maps for these periods (not shown) indicates two different atmospheric circulation patterns. A high pressure cell south of the Alaska Peninsula was the dominant feature of the earlier period, whereas the more recent period was characterized by an increased cyclonic activity in the Bering Sea.

Unlike the early winter, the overall correlation coefficient between meridional wind components at Nikolskoe and Cold Bay in the late winter is close to zero (r = -0.05).

Nevertheless, there does exist some common elements in their variability such as a simultaneous regime shift in 1977. The anomalous winds at Nikolskoe changed from predominantly southerly in the late 1960s to northerly in the late 1970s and early 1980s. In the subsequent years the winds were increasingly southerly. This upward trend during 1977-2002 was statistically significant at $p = 0.04$. It is also possible to interpret these long-term variations as step-like transitions with two shift points. The first shift occurred in 1977 when the northerly winds were the strongest over the period examined here. It set the regime of predominantly northerly winds that lasted through 1988. The second shift, which set the regime of anomalous southerly winds, occurred in 1989 when the southerly winds were the strongest. The differences in meridional winds between these three regimes (1962-1976, 1977-1988, and 1989-2003) are statistically significant at $p = 0.03$ for both shift points. At Cold Bay, meridional winds also experienced a regime shift from northerly in 1968-1976 to southerly in 1977-1982, which was statistically significant at $p = 0.001$. The trend toward more southerly winds from 1983 to 2002 is significant at $p = 0.07$.

The wind stress at Nikolskoe correlates with the zonal wind component at $r = -0.49$, $p < 0.01$. The stormiest 9-yr period, 1969-1977, was also a period of strong easterly winds associated with an enhanced cyclonic activity to the south of this region. In the subsequent years the wind stress index was mainly below the long-term average value, with one prominent exception in 1984. No obvious trends or regime shifts are evident in wind stress at Cold Bay.

The correlation coefficient between SAT at Nikolskoe and the zonal wind component is $r = -0.34$ ($p < 0.05$). The correlation is stronger ($r = -0.58$, $p < 0.005$)

between the SAT and the West Pacific (WP) teleconnection index, which characterizes the strength of the mid-tropospheric westerly winds over the western North Pacific (Wallace and Gutzler 1981). The WP pattern is one of the primary modes of low-frequency variability over the Northern Hemisphere. During winter, the pattern consists of a north-south dipole of geopotential height anomalies, with one center located over the Bering Sea and another broad center of opposite sign covering portions of southeastern Asia and the low latitudes of the extreme western North Pacific. The 500-hPa height anomalies averaged over the Bering Sea (55˚-65˚N, 170˚E-160˚W) correlate with SAT at Nikolskoe at $r = 0.74$, $p < 0.001$. Positive (negative) height anomalies in this center translate into weaker (stronger) advection of cold Siberian air to the western Aleutians region. For example, the cold period of 1998-2002 is associated with a substantial decrease of 500-hPa heights over the Bering Sea during those years.

SAT variations at Cold Bay reflect a well-known shift in the phase of the PDO around 1977 (e.g., Hare and Mantua 2000). As in the eastern Bering Sea and along the west coast of North America, the period of 1970-1976 at Cold Bay was very cold. If these years were removed from the time series, the SAT variance would have reduced by more than 30%. The overwhelming majority of the years since 1977 were warmer than normal, with a notable exception of 1999. The cold period of 1970-1976 was associated with strong northerly winds; however, another period of equally strong northerly winds, 1983-1988, did not result in any noticeable decline in SAT. These two periods are substantially different in the overall pattern of atmospheric circulation over the North Pacific. During 1970-1976, there was anomalous upper atmospheric ridging over the central North Pacific extending far north into the Bering Sea. Northerly wind anomalies along its

eastern periphery brought cold Arctic air to the eastern Aleutians. In contrast, the period of 1983-1988 was characterized by an anomalously low pressure center south of Alaska Peninsula, with Cold Bay being on the north-west side of this center. This cyclonic activity pumped warm Pacific air northward into Alaska, where temperatures were well above normal, hence even though the anomalous winds at Cold Bay were northwesterly, the SAT anomalies tended to be slightly above normal.

April – May (Fig. 8, Bottom Panel)

In spring, the storm track moves northward and westerly winds and Nikolskoe and Cold Bay become as frequent as easterly winds. The correlation coefficient between the zonal wind components at these two locations in April-May is $r = 0.54$. Both locations experienced mostly easterly winds in the early and mid-1990s, with a switch to more westerly winds in 1998. Since then, zonal wind anomalies were consistently westerlies at Nikolskoe, but not at Cold Bay.

Meridional winds at these two locations are correlated at -0.49. At Nikolskoe, there is a strong negative trend from the early 1960s, with their southerly wind anomalies, to the late 1970s and early 1980s, when northerly winds prevailed. The significance of the trend is $p = 0.001$ when the data from 1962-1984 is used for its estimate. At Cold Bay, the anomalous meridional winds were mostly northerly in 1984-1996, and mostly southerly in 1997-2003. The difference between these two periods is significant at $p = 0.06$.

Although it is not completely appropriate to compare 2-month to 3-month statistics, it is interesting to note that the long-term values of wind stress in April-May are much lower than in November-December and January-March. The interannual variability of the

wind stress index is also noticeably lower during this season. There is one period at Cold Bay that stands out, 1998-2000, when the wind stress showed a dramatic decrease from its maximum value in 1998 to its minimum value in 2000.

The interannual SAT variability at Nikolskoe in spring is also much lower than that in the previous two seasons considered here. This reduced variability makes the warming trend from the late 1970s through mid-1990s more noticeable. The significance of the trend from 1976-1997 is 0.001. At Cold Bay, the SAT variability in spring is quite similar to that in the late winter (r = 0.59). One noticeable difference is that the cooling in the mid-1980s in spring was more pronounced.

TREND ANALYSIS

This analysis was conducted for the period 1956-2002. The reason for choosing 1956 as the starting point is that the winter of 1956 marked an abrupt increase in SAT at Nikolskoe (55.2N, 166.0˚E) as seen in Fig. 9, top graph. The cold period in the early 1950s is not consistent with the SAT composite map (Fig. 6f), given that three years in the composite were 1950, 1952, and 1955. To examine this period further we extracted mean winter (DJF) SATs from the NCAR/NCEP Reanalysis dataset (Kalnay et al. 1996) for the grid point 55˚N, 165˚W, closest to Nikolskoe. The two time series (Fig. 9) match almost perfectly for the period 1956-2002 with the correlation coefficient $r = 0.94$. For the period 1949-1955, however, the SAT anomalies in the grid point were mostly opposite to those in Nikolskoe. This inconsistency may be due to either a problem with the data quality or a result of complex regional circulation patterns that produced the negative SAT anomaly centered over the northern Sea of Okhotsk in Fig. 6f. Given the uncertainty with the earlier part of the SAT record, we excluded it from our analysis.

Fig. 10 shows the trend maps for three meteorological variables presented in the form of their correlation with the time axis (years). A prominent feature of the map for 500-hPa heights (Fig. 10 top panel) is the center of negative correlations ($r < -0.4$) over the Bering Sea. It suggests that over the period 1956-2003, troughing in the mid-troposphere increased substantially in this area. It also suggests an increase in cyclonic activity at the sea level, since the atmosphere over the North Pacific and the Bering Sea is nearly barotropic (see Fig. 5 b,c and 6 b,c). The trends in meridional wind (middle panel of Fig. 10) are consistent with this interpretation, showing an increase of northerly winds over the western Bering Sea and southerly winds over Alaska. The reaction of SATs to

these changes in atmospheric circulation is a cooling trend in the western Bering Sea including the western and central Aleutians and warming in the Gulf of Alaska and eastern Bering Sea (Fig. 10 bottom panel).

The time series of winter SAT at Nikolskoe (Fig. 9) suggests that the strong cooling trend in this area is accompanied by changes in the interannual variability of SAT. Thus, from the late 1960s through the early 1980s, the variability in winter SAT values was relatively small. In the later years the magnitude of the both the positive and negative SAT anomalies kept rising. The top panel in Fig. 11 illustrates the spatial characteristics of these changes in the interannual variability. It shows the distribution of the difference in mean winter (Nov-Mar) SAT variance between1986-2002 and 1965-1985 (in per cent). The zero line, which separates the areas where the variance increased from the areas where it decreased, crosses the Alaska Peninsula. West of that line, along the Aleutian chain, the degree of that increase becomes more and more substantial reaching more than 200% in the area between the Commander and Near Islands. In contrast, in the coastal waters off British Columbia and southeast Alaska, this variance decreased more than 50%.

The middle map in Fig. 11 shows the trends (expressed as the correlation with time) in the intra-seasonal (month-to-month) variability in SATs for the cold (November through March) season. This variability was calculated as an average of squared differences of mean monthly SATs between consecutive months, i.e., November-December, December-January, January-February, and February-March. It indicates whether the season was relatively homogeneous or characterized by sharp changes in SAT from month to month. The spatial pattern of trends in this characteristic (Fig. 11,

middle map) shows a familiar east-west difference in the 50-60˚N latitudinal band, similar to that for the interannual variance. As in Fig. 11 (top map), the zero line (no trend) again crosses the Alaska Peninsula. In the areas west of this line, the correlation coefficients are increasingly positive reaching the 0.05 significance level in the western Aleutians. To the east of that line the correlation coefficients are negative with the minimum in the eastern Gulf of Alaska, indicating a statistically significant decrease in the intra-seasonal variance in this region.

To further examine the details of that intra-seasonal variability we calculated the linear trends for each of 12 monthly time-series of SAT in Nikolskoe. It turned out that the trends are insignificant for all the month except January (-0.28˚C/decade, significant at $p < 0.05$) and November (+0.25˚C/decade, $p < 0.05$). SAT variations for these two months along with the SAT difference between them are shown in Fig. 12. The trend in the November-January differences is even more impressive: from 2.4˚C at the beginning of the time series to 4.8˚C at the end, or 0.52˚C/decade. Particularly high values of SAT changes from November to January were observed in 1985-1995, when they averaged 5.4˚C. In comparison, the average change in the SAT between these two months in 1956-1971 was only 2.7˚C, or half of that during 1985-1995. The spatial pattern of trends in the November-January SAT difference (Fig. 11, bottom map) closely resembles the pattern for the month-to-month SAT variability (Fig. 11, middle map), which suggests that this variability is primarily determined by the opposite temperature trends in these two months.

REGIME SHIFTS

In the past three decades or so, the climate of the North Pacific experienced two regime shifts – in 1977 and 1989 – that had substantial impacts on marine ecosystems (Hare and Mantua, 2000). The shift of 1977 is well documented (as reviewed by Miller et al. 1994). Its characteristics include deepening of the Aleutian low, southward displacement of the Pacific storm track, lower SST and a deeper ocean mixed layer across the central North Pacific, and higher SST along the North American coast and Alaska, along with changes in a host of other environmental and biological indices (Trenberth 1990; Ebbesmeyer et al., 1991; Trenberth and Hurrell 1994; Miller et al. 1994; Nakamura 1997). The 1989 regime shift in the North Pacific is more prominent in biological records than in indices of Pacific climate (McFarlane 2000). In this section we briefly discuss the transitions in the SAT anomaly patterns associated with these two regimes, with a focus on the Aleutian Islands and the winter season when the Aleutian low reaches its maximum development.

Fig. 13a shows the distribution of normalized SAT anomalies prior to the regime shift of 1977. It represents a typical negative PDO pattern with positive temperature anomalies in the central North Pacific and negative anomalies along the west North American coast. These two areas are separated by a high-gradient zone in SAT anomalies. In the Gulf of Alaska and eastern Bering Sea negative SAT anomalies exceed one standard deviation (which is statistically significant at $p < 0.03$ using one-tail Student's t-test). For Kodiak, for example, the period 1971-1976 was the coldest 6-yr stretch since the continuous temperature record began in 1899. Farther west, however, the

magnitude of negative SAT anomalies drastically decreases and in the western Aleutians they are close to zero.

The SAT anomaly pattern in 1977-1988 (Fig. 13b) is opposite to that in 1971-1976 (Fig. 13a). The most significant positive deviations from the long-term mean values (exceeding the 0.05 significance level of 0.66) were observed over southwest Alaska. In Kodiak, this period was extremely warm (since the data for 1946 are missing it is not clear whether or not it was warmer than 1935-1946). It is not surprising therefore that the regime transition around 1977 in Kodiak was extremely sharp (Fig. 14, top chart), with the significance level $p < 0.01$ (two-tailed t-test). In Cold Bay (Fig. 14, middle chart), despite the cold winter of 1980, the shift was still significant at $p = 0.01$. Farther west, however, as seen in Fig. 13c, the magnitude of the shift is diminished. In Adak (Fig. 14, bottom chart), there was little sign of a shift around 1977.

The SAT anomaly map for 1989-1997 (Fig. 13d) does not resemble a PDO pattern, and hence, this regime is not a return to the pre-1977 conditions. Although the central North Pacific warmed up appreciably, SAT anomalies along the west coast of North America did not reverse their sign. Negative SAT anomalies of less than 0.2 standard deviations were observed in the western Gulf of Alaska and central and northern parts of the Bering Sea.

The SAT difference map between 1989-1997 and 1977-1988 (Fig. 13e) shows a resemblance to the negative PDO pattern. The maximum rate of cooling was in southwestern Alaska and adjacent waters, where the difference between mean SAT values in these two periods was statistically significant at $p = 0.01$. While the magnitude

of positive SAT anomalies in Cold Bay somewhat decreased in 1989-1997, the change was not statistically significant.

Winter SATs in Nikolskoe (Fig. 9) indicate a drop for the western Aleutians not in 1989, but two years earlier. The spatial distribution of the normalized SAT anomalies for 1987-2002 (Fig. 13f) shows that the cooling was centered in the western Bering Sea where negative SAT anomalies reached 0.6 standard deviation, a value beyond the 0.05 significance level (one-tail t-test). This period was appreciably colder than the 1951-2000 climatology in the western Aleutians as well, whereas waters off British Columbia and eastern Gulf of Alaska were warmer than normal.

EAST – WEST CONTRASTS

The analysis of meteorological time series at Nikolskoe and Cold Bay has demonstrated that the western and eastern Aleutians are markedly different in terms of patterns of climate variability in these two regions. Although both regions are affected by the Aleutian low, its effects are translated differently into their regional climate variability. The SAT fluctuations in the eastern Aleutians have much in common with those in the eastern Bering Sea and eastern North Pacific; they clearly track major changes in the overall Pacific climate associated with the PDO. The PDO signal becomes weak or nonexistent in the western Aleutians. Instead, SAT variations in this region relate strongly to the WP pattern.

A number of maps presented in this study suggest an overall opposition of climate fluctuations in the western and eastern parts of the area of Steller sea lion habitat. For example, Fig. 6f shows that during years of high NPI values (weak Aleutian low), SAT anomalies are positive in the western and central Aleutian Islands and negative in the eastern Gulf of Alaska. At the one point SAT correlation map for Nikolskoe (Fig. 7a), the correlation coefficient changes its sign in the Gulf of Alaska. The correlation contours on this map and a similar map for Cold Bay (Fig. 7b) are packed relatively tight at the central and eastern Aleutian Island suggesting an existence of a transition zone in this region. The directions of linear SAT trends (Fig. 10c) are opposite east and west of approximately 165˚W. The opposition is also evident with regards to changes in the interannual and month-to-month SAT variances (Fig. 11), with the zero line crossing the Alaska Peninsula at approximately 155˚W.

The existence and location of east-west transition zone(s) were determined using the following method. Two sets of spatial correlation functions for winter (DJF) SAT were computed along the 52.5˚N parallel. For the western set of base points, the correlation functions were calculated for points to the east of the base points and vice versa. In Fig. 15a both sets are plotted together. The idea is to find the centers ("attractors") where the correlation functions from different base points tend to reach their minima. Also, these attractors should come in pairs, so that the correlation functions calculated in opposite directions from these attractors should reach their minima at their counterpart's attractor. There are two pairs of such attractors in Fig. 15a. In the first pair, a correlation function calculated from 105˚W westward reaches its minimum marked as A1 at 175˚W, and a correlation function from this point eastward reaches its minimum at 105˚W (A2). This pair of attractors, A1-A2, represents a quasi-permanent teleconnection dipole. Another dipole, B1-B2, is formed by a pair of correlation functions with the base points at 145˚E and 105˚W. It less pronounced than A1-A2, but the correlation coefficients for its two centers are statistically significant. The correlation functions for A1 and A2 cross each other above the zero line, which indicates some asymmetry between them. This also suggests a broad transition zone between these two centers of opposite SAT fluctuations centered at about 150˚W. The correlation functions for B1 and B2 cross each other at the zero line suggesting a more narrow transition zone at 170˚W. The sharpness of this transition zone can be confirmed by calculating correlation coefficients between the successive grid points separated by 10˚ longitude. The line connecting those correlation coefficients (Fig. 15b) has a minimum at 170˚W.

SUMMARY

The climatological analysis presented above demonstrates that, although the mean climate is similar throughout the Aleutians, the interannual and longer-term variability patterns have little in common for the western and eastern islands. The climatological transition zone between these two regions lies at about 170˚W. A broader, but statistically more significant transition zone in terms of the east-west SAT opposition is found at about 150˚W.

The climate of the western Aleutians was characterized by a cooling trend from 1956-2002. This trend was consistent with the changes in atmospheric circulation brought about by the overall strengthening of the Aleutian low. One of the manifestations of this circulation trend was the decline of cyclonic activity along secondary storm track into the western Bering Sea. During the 1950s and 1960s, when the Aleutian low was weak, storms often propagated northeastward along the Asian coast bringing warm air to the western Aleutians. As the Aleutian low strengthened, the storms tended to track farther south. The deepening of the Asian trough aloft translated into more frequent outbreaks of cold Siberian air to the western Aleutians. The relationship between the strength of the Aleutian low and SATs in the western Aleutians does not seem to be linear. During periods of an extremely strong Aleutian low, as expressed by the NP index, the tongue of positive SAT anomalies extends from the Gulf of Alaska far enough westward to reach the western Aleutians.

The eastern Aleutians, as for most of the North Pacific, experienced a climate shift in 1977. This shift was manifested strongly in the vicinity of Kodiak Island, where temperatures jumped from a record low level in 1971-1976 to a record (or near record)

high level in1977-1988. In Cold Bay, at the tip of Alaska Peninsula, the shift was also significant at $p = 0.01$, but was much weaker further west, becoming near zero at the dateline.

The climate shift of 1989 was also much more pronounced in the eastern than in the central and western Aleutians. This shift, however, was not a return to the pre-1977 conditions, but rather a moderation of a very warm period of 1977-1988. The western Aleutians experienced a shift to predominantly negative SAT anomalies in 1987. This shift can be considered as a major component of an overall negative trend in the region.

The cooling trend in the western Aleutians was accompanied by a trend toward more variable SAT, both on inter- and intra-annual time scales. In the past two decades or so, the magnitude of mean winter (DJF) SAT anomalies of both signs saw a steady increase. During 1986-2002, the variance of winter SATs was more than twice that during 1965-1985. The opposite situation occurred in southeast Alaska, where the SAT variance decreases by about 50%. The spatial pattern of changes in the intra-seasonal variability for the cold (November-March) season is similar: it increased for the western Aleutians and decreased for the southeast Alaska. Much of the increase in the intra-seasonal variability for the western Aleutians is associated with the warming trend in November and cooling trend in January. As a result, the rate of seasonal cooling from November to January is doubled since the late 1950s.

We hypothesize that this trend toward higher SAT variability in the western Aleutians may have contributed to the decline in the Steller sea lion population of the region. The SAT variability could have had direct impacts, for example, by increasing the physiological stress on juvenile sea lions. In addition, or instead, the SAT variability may

be associated with other aspects of the physical ocean-atmosphere system that ultimately help determine the production of prey for sea lions and their competitors. The eastern stock (east of 144˚W) show no sign of decline, and the fact that SAT variability in this area decreased over the same period provides some credibility to the hypothesis. Therefore, while climate is just one of a host of potential influences, our result of a prominent west-east difference in SAT variability suggests that climate changes may have been instrumental in the decline of the western Aleutian stock, and the increase in the eastern Gulf of Alaska stock.

ACKNOWLEDGEMENTS

We thank three anonymous reviewers for their detailed comments and suggestions. This publication is funded by the Joint Institute for the Study of the Atmosphere and Ocean (JISAO) under NOAA Cooperative Agreement No. NA17RJ1232, Contribution No. 1022. The research was also sponsored by NOAA's Steller Sea Lion Research program and is contribution FOCI-L526 to Fisheries-Oceanography Coordinated Investigations. This is NOAA's Pacific Marine Environmental Laboratory Contribution No. 2625 and GLOBEC Contribution No. 430.

REFERENCES

Bayley, G.V., and Hammersley, J.M. (1946) The effective number of independent observations in an autocorrelated series. *J. Roy. Stat. Soc*., **B8**, 184-197.

Benson, A.J., and Trites, A.W. (2002) Ecological effects of regime shifts in the Bering Sea and eastern North Pacific Ocean. *Fish and Fisheries*, **3**, 95-113.

Braham, H. W., Everitt, R. D., and Rugh, D. J. (1980) Northern sea lion decline in the eastern Aleutian Islands. *Journal of Wildlife Management*, **44**, 25-33.

Barsugli, J. J., and Battisti, D. S. (1998) The basic effects of the atmosphere–ocean thermal coupling on midlatitude variability. *J. Atmos. Sci.,* **55**, 477–493.

Chang, E.K.M., and Fu, Y. (2002) Interdecadal Variations in Northern Hemisphere Winter Storm Track Intensity. *J. Climate,* **15**: 642–658.

Cohen, J., and Cohen, P. (1983). *Applied multiple regression/correlation analysis for the behavioral sciences.* Hillsdale, NJ: Erlbaum.

Ebbesmeyer, C.C., Cayan, D.R., McClain, D.R., Nichols, F.H., Peterson, D.H. and Redmond, K.T. (1991) 1976 step in Pacific climate: Forty environmental changes between 1968-1975 and 1977-1984. *In: J.L. Betancourt and V.L. Tharp (Eds.) Proceedings of the 7th Annual Pacific Climate (PACLIM) Workshop, April 1990. California Department of Water Resources. Interagency Ecological Study Program Technical Report 26* : 115-126.

Flatau, M., Talley, L., and Musgrave, D. (2000) Interannual Variability in the Gulf of Alaska during the 1991–94 El Nino. *J. Climate,* **13**: 1664–1673.

Hare S.R., and Mantua, N.J. (2000) Empirical evidence for North Pacific regime shifts in 1977 and 1989. *Progr. Oceanog.,* **47**: 103-146.

Kalnay, E. and Coauthors (1996) The NCEP/NCAR reanalysis 40-year project. *Bull. Amer. Meteorol. Soc.,* **77**: 437-471.

King, J.R., Ivanov, V.V., Kurashov, V., Beamish, R.J., and G.A. McFarlane (1998) General circulation of the atmosphere over the North Pacific and its relationship to the Aleutian Low. *North Pacific Anadromous Fish Commission Doc. No. 318. Department of Fisheries and Oceans, Science Branch – Pacific Region, Pacific Biological Station, Nanaimo, BC, Canada,* : 18 p.

Kistler, R., E. Kalnay, W. Collins, S. Saha, G. White, J. Woollen, M. Chelliah, W. Ebisuzaki, M. Kanamitsu, V. Kousky, H. van den Dool, R. Jenne, M. Fiorino (2001) The NCEP-NCAR 50-Year Reanalysis: Monthly Means CD-ROM and Documentation. Bull. *Amer. Meteor. Soc*., **82**: 247-268.

Loughlin, T. R., and York, A. E. (2000) An accounting of the sources of Steller sea lion mortality. *Mar. Fish. Rev*. **62:** 40-45.

Mantua, N.J., Hare, S.R., Zhang, Y., Wallace, J.M., and Francis, R.C. (1997) A Pacific interdecadal climate oscillation with impacts on salmon production. *Bull. Amer. Meteorol. Soc.,* **78**: 1069-1079.

McFarlane, G. A., King, J. R. and Beamish, R. J. (2000) Have there been recent changes in climate: Ask the fish. *Progr. Oceanog.,* **47**: 147-169.

Miller, A. J. and Schneider, N. (2000) Interdecadal climate regime dynamics in the North Pacific Ocean: theories, observations, and ecosystem impacts. *Progr. Oceanog.,* **47**: 355–379.

Miller, A.J., Cayan, D.R., Barnett, T.P., Graham, N.E., and Oberhuber, J.M. (1994) The 1976-77 climate shift of the Pacific Ocean. *Oceanography,* **7**: 21-26..

Nakamura, H., Lin, G. and Yamagata, T. (1997) Decadal climate variability in the North Pacific during the recent decades. *Bull. Amer. Meteorol. Soc.,* **78**: 2215–2225.

Niebauer, H.J. (1998) Variabillity in Bering Sea ice cover as affected by a regime shift in the Pacific in the period 1947-1996. *J. Geophys. Res.,* **103**: 27717-27737.

NRC (2003) *The Decline of the Steller Sea Lion in Alaskan Waters: Untangling Food Webs and Fishing Nets*. Committee on the Alaska Groundfish Fishery and Steller Sea Lions, National Research Council, National Academies Press, 204 pp.

Overland, J. E., Adams, J.M., and Bond, N.A. (1999) Decadal variability of the Aleutian Low and its relation to high-latitude circulation. *J. Climate,* **12**: 1542-1548.

Schneider, N., Miller, A.J. and Pierce, D.W. (2002) Anatomy of North Pacific Decadal Variability. *J. Climate,* **15**: 586–605.

Seckel, G. R. (1993) Zonal gradient of the winter sea level atmospheric pressure at 50 N: an indicator of atmospheric forcing of North Pacific surface conditions. *J. Geophys. Res.,* **98**: 22615–22628.

Springer, A.M. (1998) Is it all climate change? Why marine bird and mammal populations fluctuate in the North Pacific**.** In: *Biotic impacts of extratropical climate change in the Pacific. 'Aha Huliko'a Proceedings Hawaiian Winter Workshop,* University of Hawaii: 109-119.

Tachibana, Y., Honda, M. and Takeuchi, K. (1996) The abrupt decrease of the sea ice over the southern part of the Sea of Okhotsk in 1989 and its relation to the recent weakening of the Aleutian low. *J. Oceanogr. Soc. Japan,* **74**: 579-584.

Trenberth, K.E. (1990) Recent observed interdecadal climate changes in the Northern Hemisphere. *Bull. Amer. Meteorol. Soc.,* **71**: 988-993.

Trenberth, K.E. and Hurrell, J.W. (1994) Decadal atmosphere-ocean variations in the Pacific. *Climate Dynamics,* **9**: 303-319.

Wallace, J.M., and Gutzler, D.S. (1981) Teleconnections in the geopotential height field during the Northern Hemisphere. *Mon. Wea. Rev*., **109**, 784-812.

York, A.E., Merrick, R.L. and Loughlin, T.R. (1996) An analysis of the Steller sea lion metapopulation in Alaska. Pp. 259-292 in *Metapopulations and Wildlife Conservation*, D.R. McCullough, ed. Island Press, Washington, D.C.

Figure Captions

Figure 1. Estimated total population of Steller sea lions in thousands (from T. Loughlin, National Marine Mammal Laboratory, personal communication).

Figure 2. Map of the Aleutian Islands.

Figure 3. Mean winter (DJF) conditions for the period 1951-2000 for a) sea level pressure (hPa), b) 500-hPa geopotential height (m), and c) storm tracks. For the storm tracks the contours (every unit) and shading (every half unit) are frequencies (number/month) of storms in each 2˚ lat by 4˚ lon rectangles. The arrows show the average direction of storm in those rectangles where the frequency is greater than 1.5/month. The length of the arrow characterizes the stability of that direction. When it equals the unit length shown in the legend, it means that all the storms passed the square in that direction. The storm track data were obtained from the Climate Diagnostic Center web site (http://www.cdc.noaa.gov/map/clim/storm.shtml).

Figure 4. The North Pacific Index, 1950-2003 (adapted from Trenberth and Hurrell, 1994). The solid line is a 5-yr running average.

Figure 5. Composite maps of a) SLP (hPa), b) SLP anomaly (standard deviations), c) 500-hPa height (m), d) 500-hPa height anomaly (standard deviations), e) storm tracks, and f) SAT anomaly (standard deviations) for 10 years with the lowest NP index during 1950-2002. The base period for anomalies is 1951-2000. Assuming that the variance has not changed over time, the anomalies in figures b, d, and f

are locally significant at the 0.05 probability level (one-tail t-test) if their magnitude exceeds 0.57.

Figure 6. Same as Fig. 4, but for 10 years with the highest NP index.

Figure 7. One-point correlation maps for winter (DJF) SATs at a) Nikolskoe and b) Cold Bay. Data: 1950-2003. Correlation coefficients exceeding |0.25| (|0.34|) are significant at the 0.05 (0.01) level.

Figure 8. Time series of zonal (u) and meridional (v) wind components, wind stress, and SAT at Nikolskoe (solid line) and Cold Bay (broken line) averaged for November-December (top panel), January-March (middle panel), and April-May (bottom panel). The horizontal lines for each time series indicate the mean values for the base period, 1961-2000.

Figure 9. Normalized (by standard deviation) mean winter (DJF) SAT anomalies at Nikolskoe (1949-2002) and the grid point 55˚N, 165˚E from the Reanalysis (1949-2003).

Figure 10. Correlation coefficients with time (years) for mean winter (DJF) a) 500-hPa height, b) meridional wind component at the 500-hPa level, and c) SAT. The correlation coefficients exceeding |0.25| are significant at $p < 0.05$.

Figure 11 a) Difference in mean winter (November-March) SAT variance between 1986-2002 and 1965-1985, in per cent, b) Correlation coefficients with time (years) for intra-seasonal (November-March) SAT variance, and c) same as b) but for the SAT difference between November and January.

Figure 12 SAT anomalies at Nikolskoe for a) January and b) November, and c) difference between these two months, 1956-2002. Straight lines are least-square linear trends.

Figure 13. Normalized mean winter (DJF) SAT anomalies for a) 1971-1976, b) 1977-1988, c) 1977-1988 minus 1971-1976, d) 1989-1997, e) 1989-1997 minus 1977-1988, and f) 1987-2002. The base period for anomalies: 1951-2000.

Figure 14. Normalized mean winter (DJF) SAT anomalies at (from top to bottom) Kodiak, Cold Bay, and Adak, Alaska.

Figure 15. a) Spatial correlation functions of winter (DJF) SAT along the 52.5˚N parallel for different base points. Solid lines are the correlation functions for the dipoles A1-A2 (thick line) and B1-B2 (thin line). The gray vertical bars indicate the transition zones between the opposite centers of the dipoles. b) Correlation coefficients along the same parallel between SATs at the pairs of grid points 5˚ east and 5˚west of the given point.

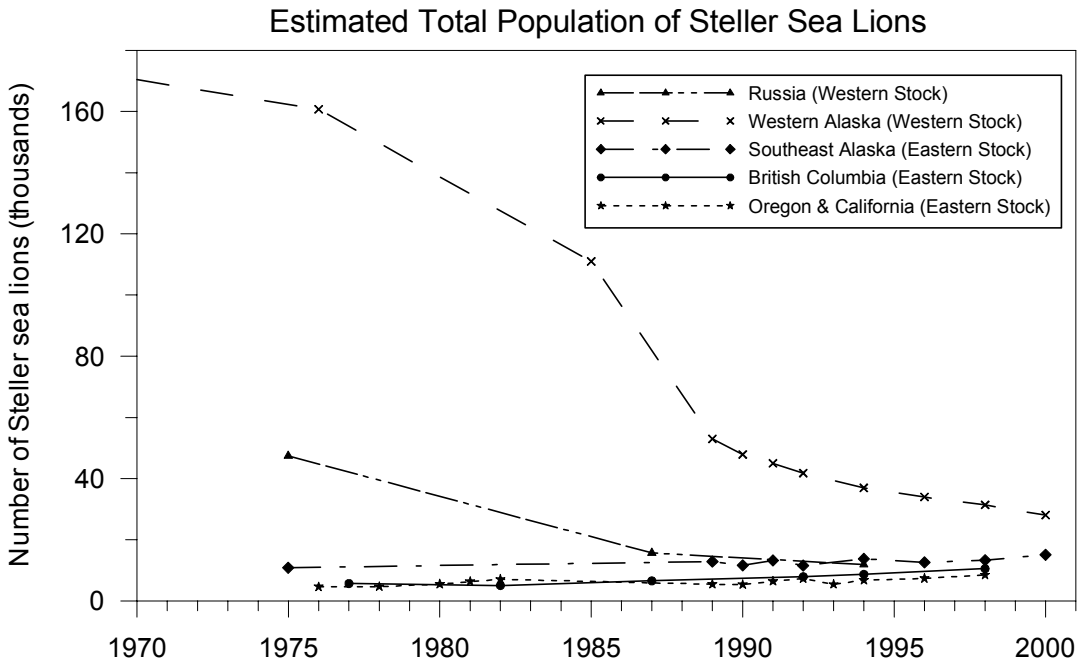

Figure 1. Estimated total population of Steller sea lions in thousands (from T. Loughlin, National Marine Mammal Laboratory, personal communication).

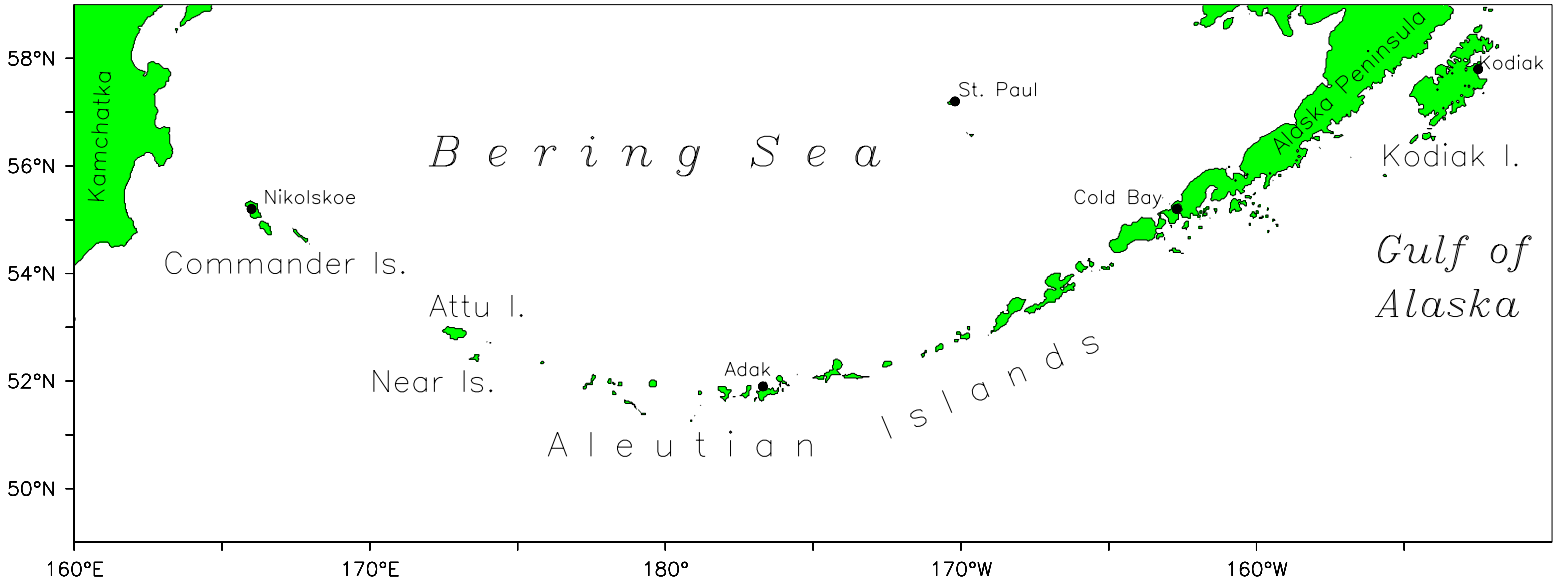

Figure 2. Map of the Aleutian Islands.

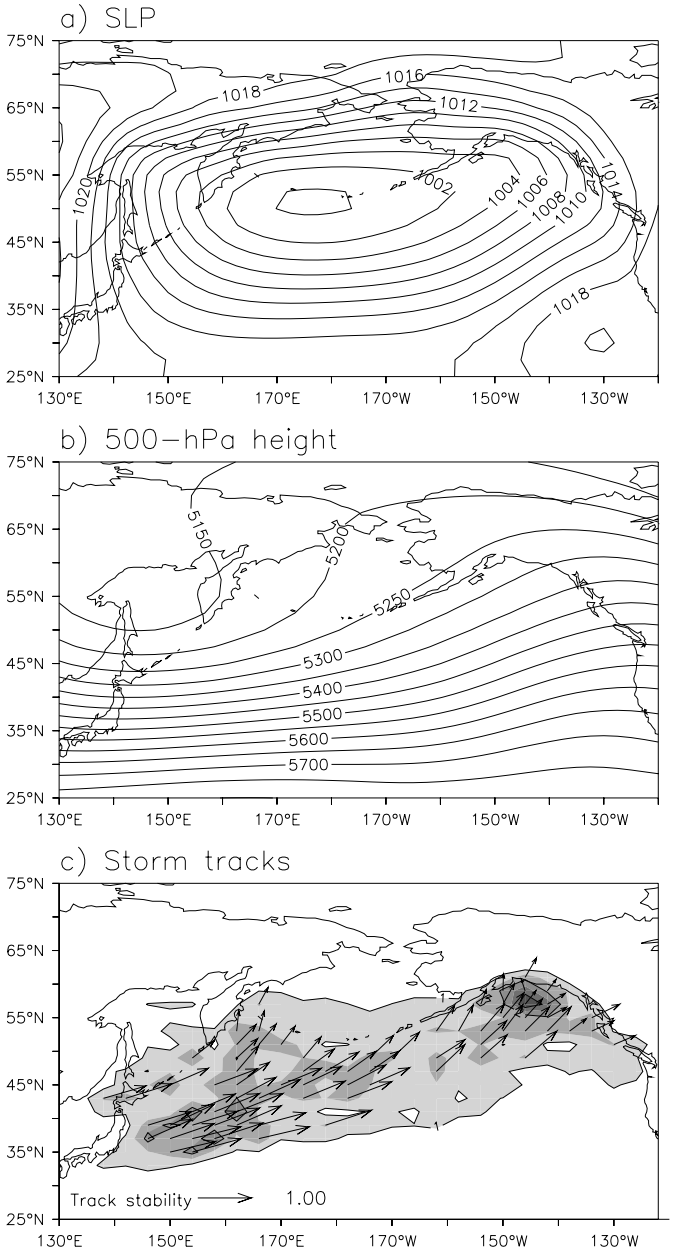

Figure 3. Mean winter (DJF) conditions for the period 1951-2000 for a) sea level pressure, b) 500-hPa geopotential height, and c) storm tracks. For the storm tracks the contours (every unit) and shading (every half unit) are frequencies (number/month) of storms in each 2˚ lat by 4˚ lon rectangles. The arrows show the average direction of storm in those rectangles where the frequency is greater than 1.5/month. The length of the arrow characterizes the stability of that direction. When it equals the unit length shown in the legend, it means that all the storms passed the square in that direction. The storm track data were obtained from the Climate Diagnostic Center web site (http://www.cdc.noaa.gov/map/clim/storm.shtml).

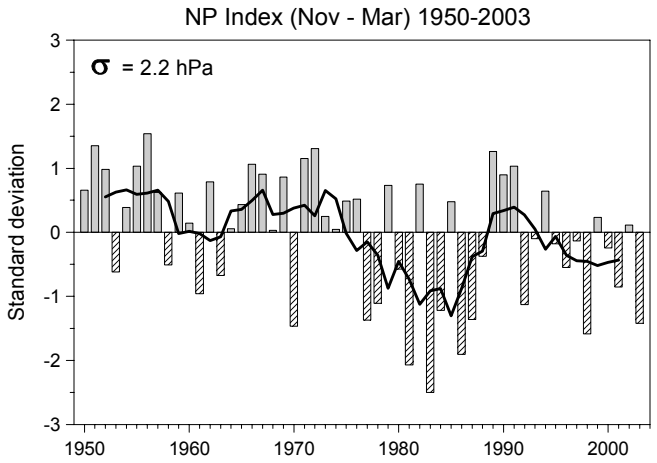

Figure 4. The North Pacific Index, 1950-2003 (adapted from Trenberth and Hurrell, 1994). The solid line is a 5-yr running average.

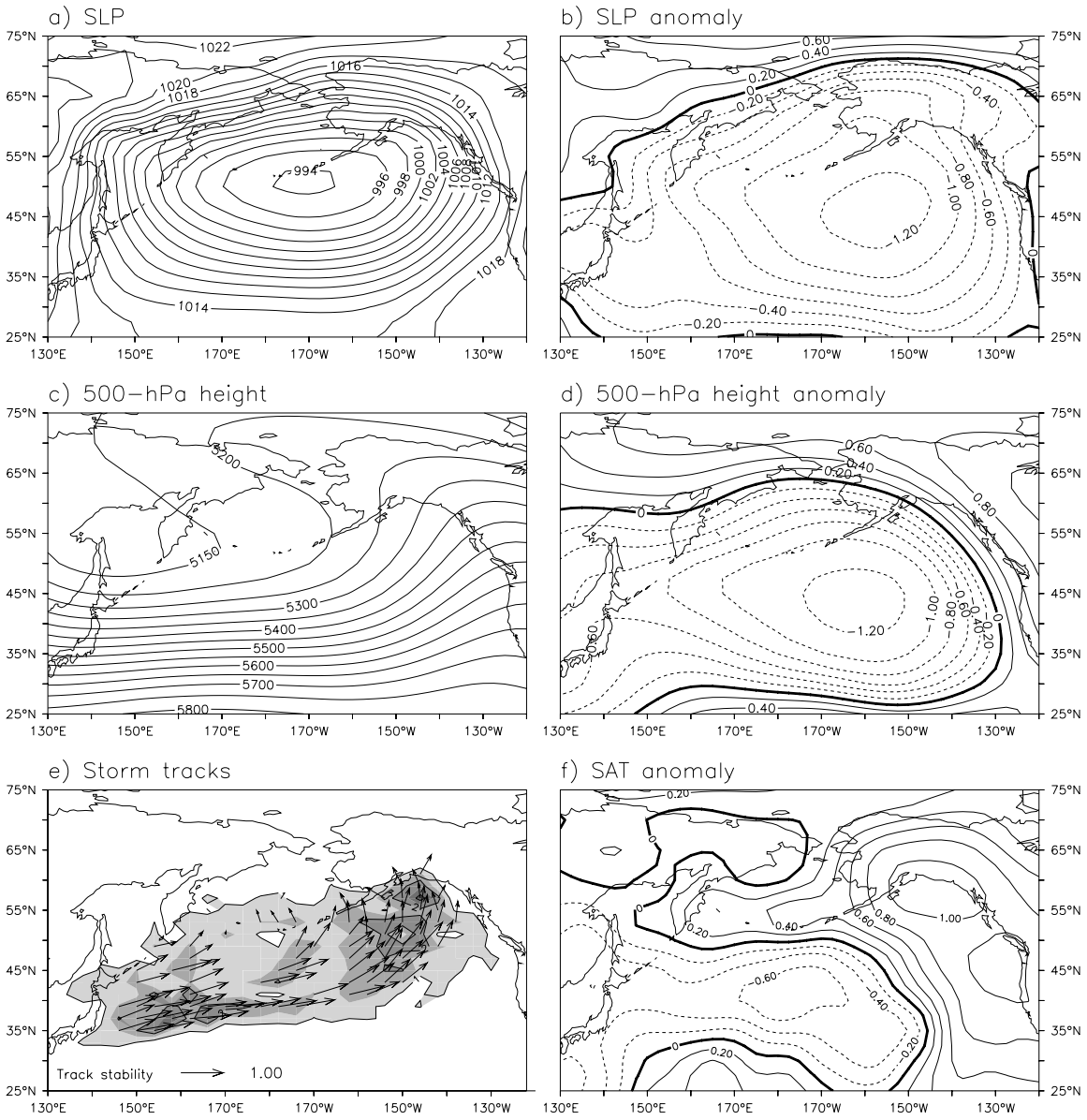

Low NPI years: 1961, 1963, 1970, 1977, 1978, 1981, 1983, 1986, 1987, 1998

Figure 5. Composite maps of a) SLP, b) SLP anomaly, c) 500-hPa height, d) 500-hPa height anomaly, e) storm tracks, and f) SAT anomaly for 10 years with the lowest NP index during 1950-2002. The base period for anomalies is 1951-2000. Assuming that the variance has not changed over time, the anomalies in figures b, d, and f are locally significant at the 0.05 probability level (one-tail t-test) if their magnitude exceeds 0.57.

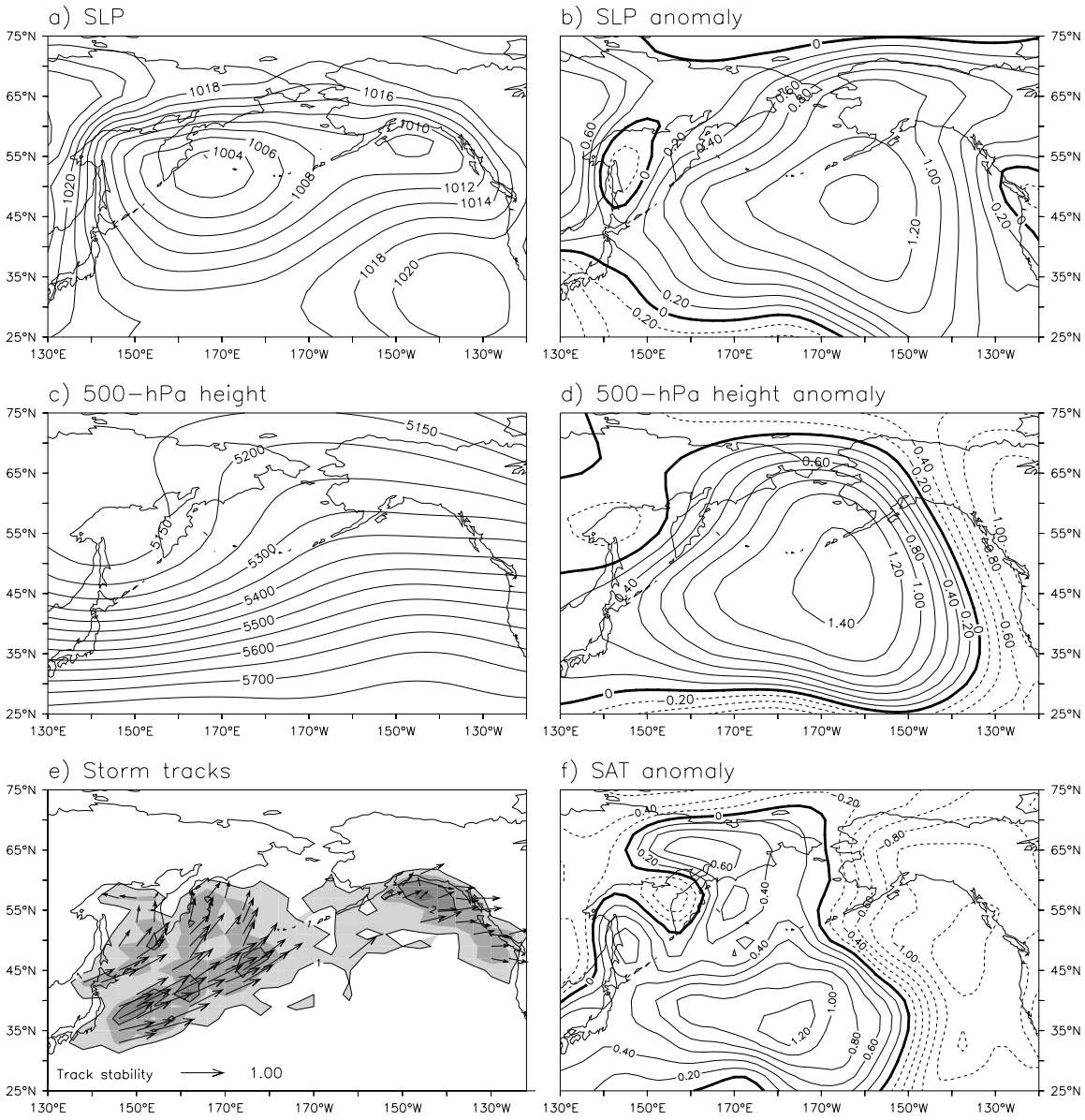

Figure 6. Same as Fig. 4, but for 10 years with the highest NP index.

.

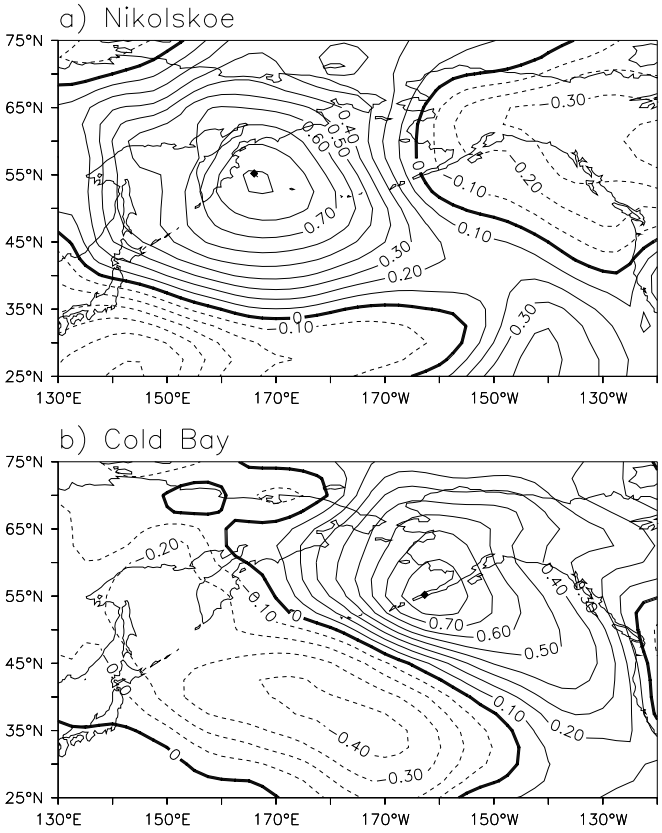

Figure 7. One-point correlation maps for winter (DJF) SATs at a) Nikolskoe and b) Cold Bay. Data: 1950-2003. Correlation coefficients exceeding |0.25| (|0.34|) are significant at the 0.05 (0.01) level.

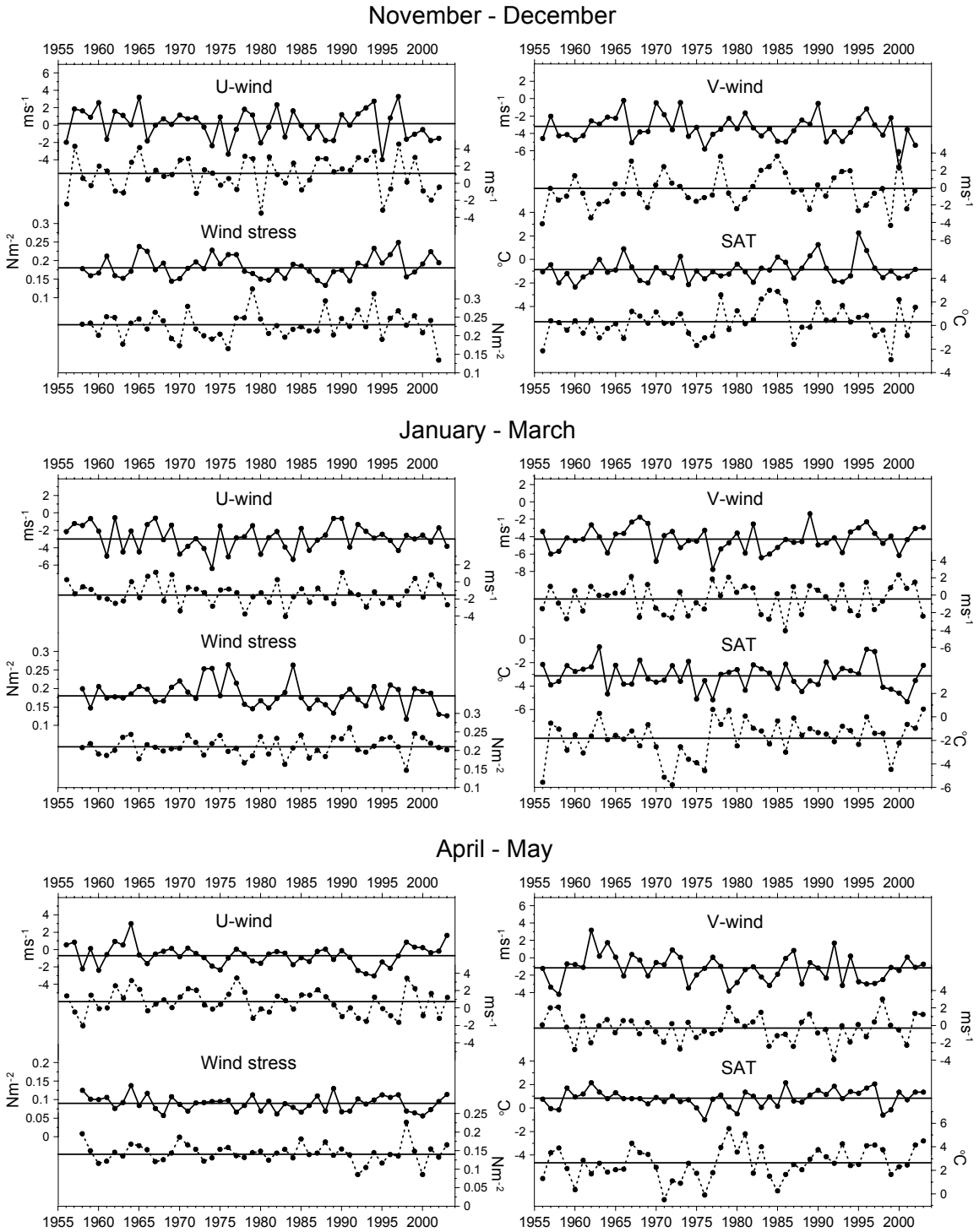

Figure 8. Time series of zonal (*u*) and meridional (*v*) wind components, wind stress, and SAT at Nikolskoe (solid line) and Cold Bay (broken line) averaged for November-December (top panel), January-March (middle panel), and April-May (bottom panel). The horizontal lines for each time series indicate the mean values for the base period, 1961-2000.

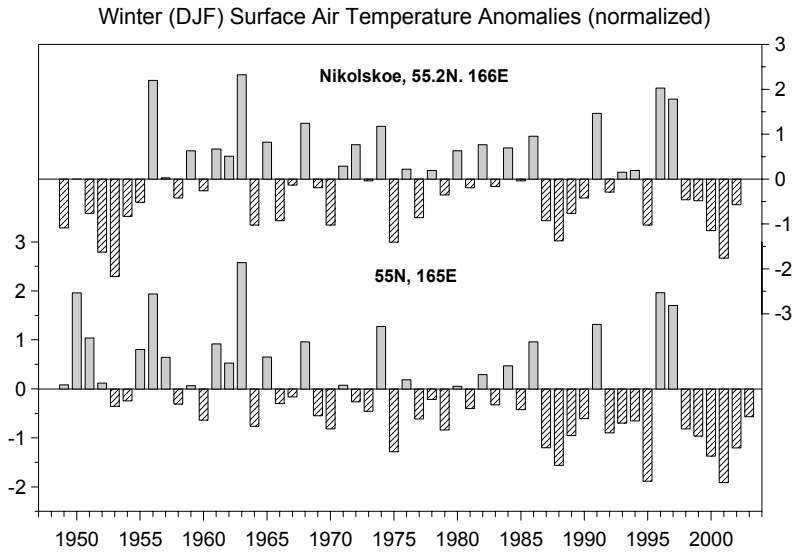

Figure 9. Normalized (by standard deviation) mean winter (DJF) SAT anomalies at Nikolskoe (1949-2002) and the grid point 55˚N, 165˚E from the Reanalysis (1949-2003).

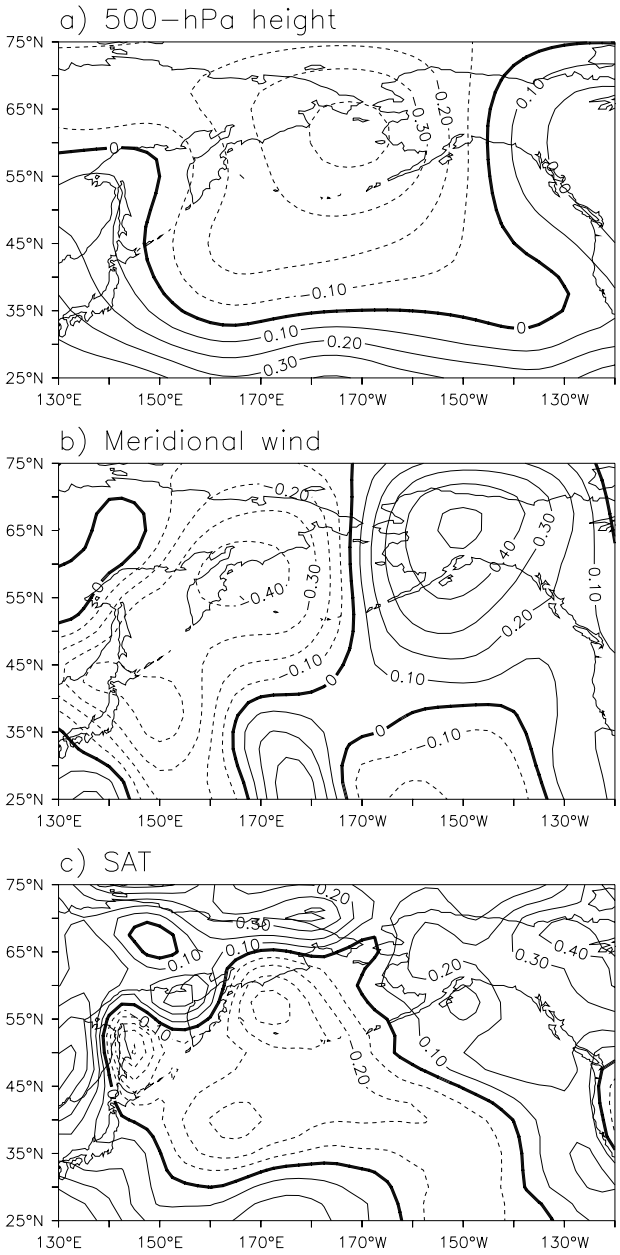

Figure 10. Correlation coefficients with time (years) for mean winter (DJF) a) 500-hPa height, b) meridional wind component at the 500-hPa level, and c) SAT. The correlation coefficients exceeding |0.25| are significant at $p < 0.05$.

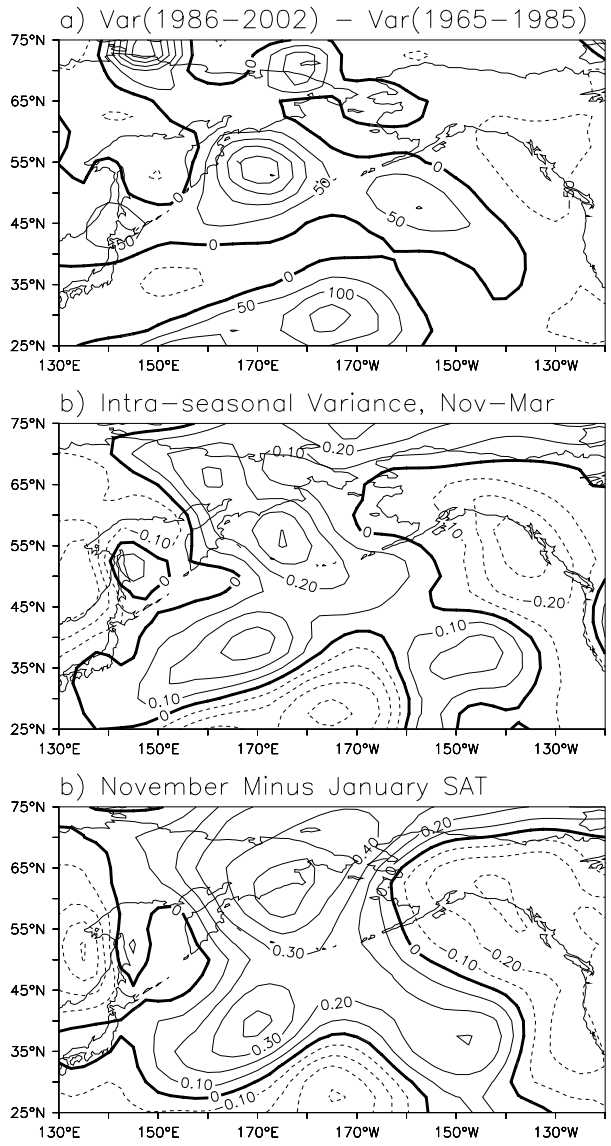

Figure 11. a) Difference in mean winter (November-March) SAT variance between 1986-2002 and 1965-1985, in per cent, b) Correlation coefficients with time (years) for intra-seasonal (November-March) SAT variance, and c) Same as b) but for the SAT difference between November and January.

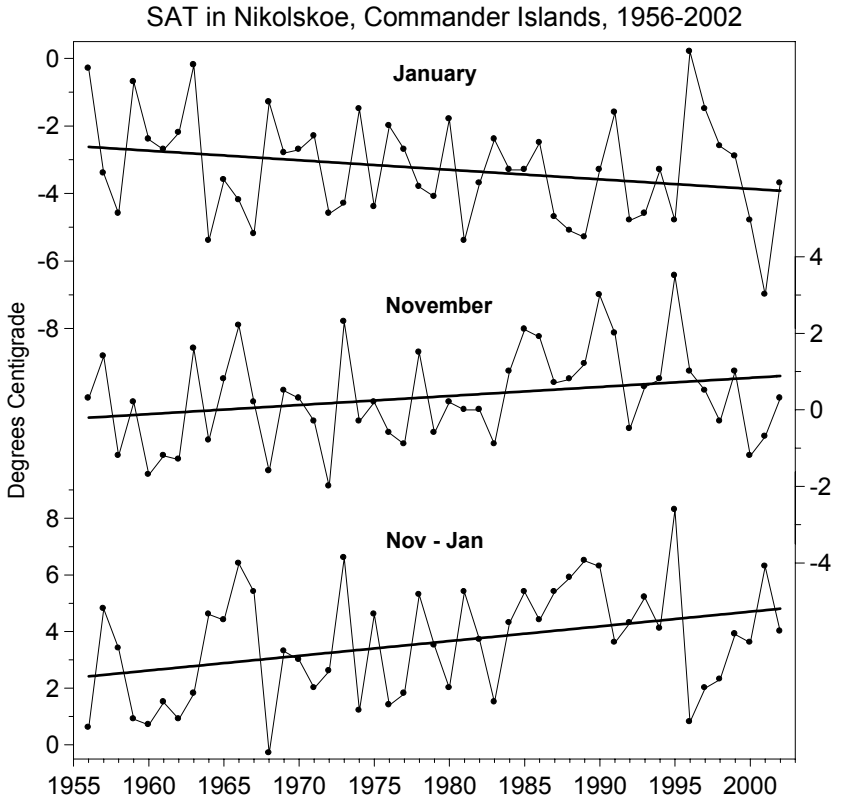

Figure 12. SAT anomalies at Nikolskoe for a) January and b) November, and c) difference between these two months, 1956-2002. Straight lines are least-square linear trends.

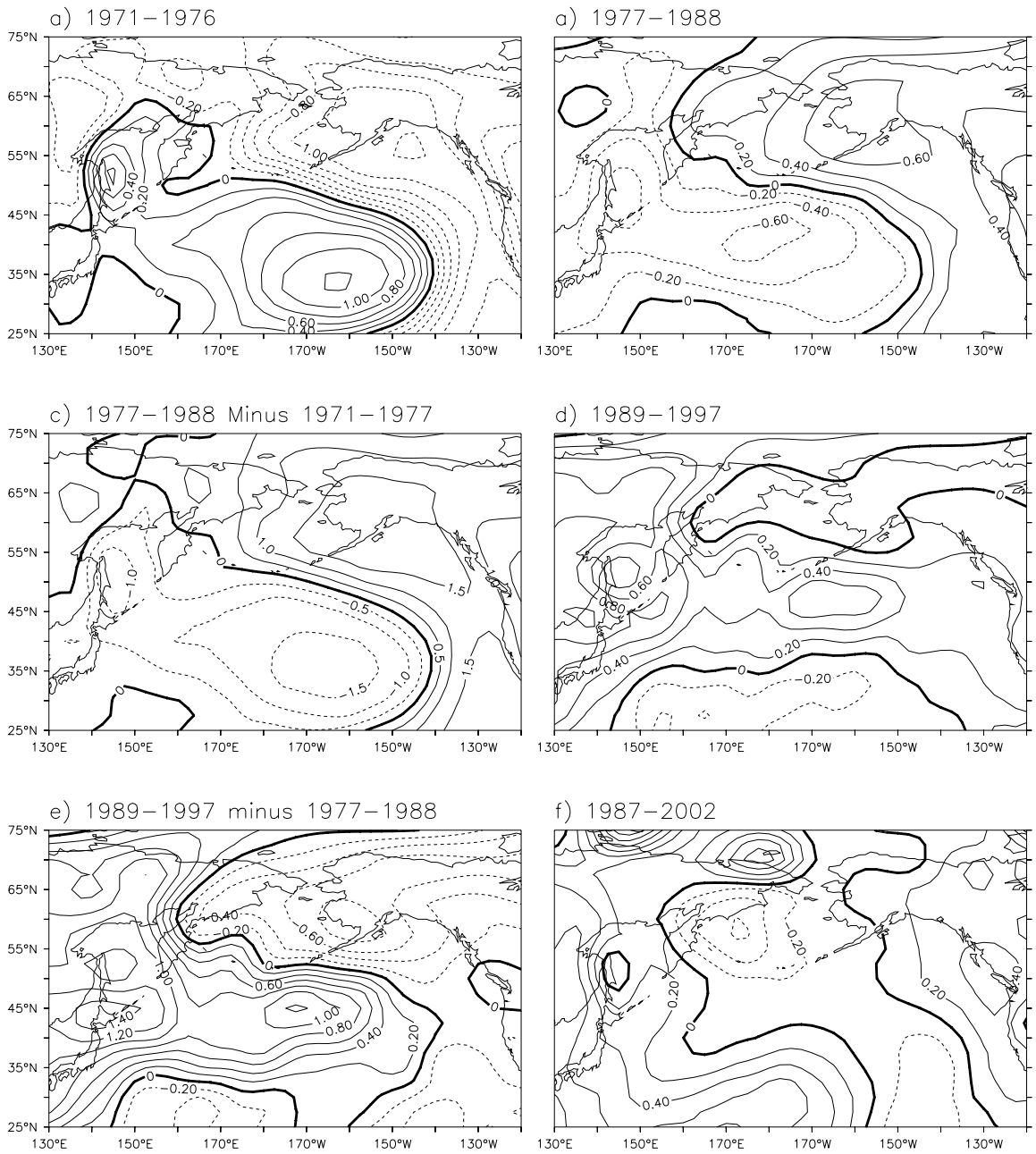

Figure 13. Normalized mean winter (DJF) SAT anomalies for a) 1971-1976, b) 1977-1988, c) 1977-1988 minus 1971-1976, d) 1989-1997, e) 1989-1997 minus 1977-1988, and f) 1987-2002. The base period for anomalies: 1951-2000.

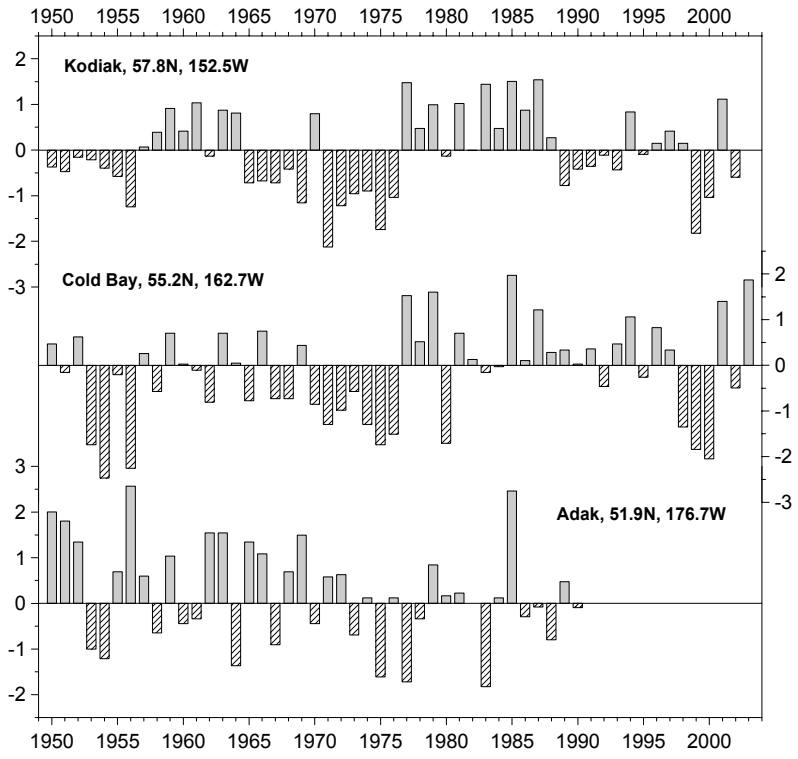

Figure 14. Normalized mean winter (DJF) SAT anomalies at (from top to bottom) Kodiak, Cold Bay, and Adak, Alaska.

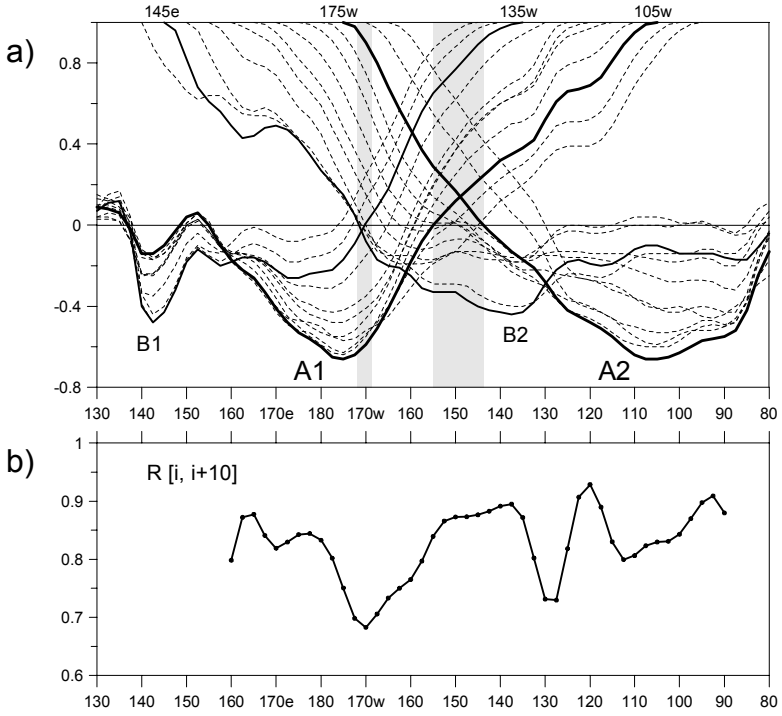

Figure 15. a) Spatial correlation functions of winter (DJF) SAT along the 52.5˚N parallel for different base points. Solid lines are the correlation functions for the dipoles A1-A2 (thick line) and B1-B2 (thin line). The gray vertical bars indicate the transition zones between the opposite centers of the dipoles. b) Correlation coefficients along the same parallel between SATs at the pairs of grid points 5˚ east and 5˚west of the given point.